JIP
Jurnal Ilmiah PLATAX
Universitas Sam Ratulangi
Terakreditasi Ristekdikti No: 28/E/KPT/2019
ISSN : 2302-3589 (Online)
E_mail : jm_platax@unsrat.ac.id

In-Silico Optimization of Macrolactin A from Sponge-Associated Bacteria and Its Derivatives as Eco-Friendly Antifoulants

Walter Balansa*[1], Riyanti[2], Jelita Siska Herlina Hinonaung[3]

[1]Department of Fishery and Maritime Technology, Politeknik Negeri Nusa Utara. Jl. Kesehatan No 1, Kepulauan Sangihe 95812, North Sulawesi, Indonesia.
[2]Faculty of Fisheries and Marine Science, Universitas Jenderal Soedirman, Jl. Dr. Soeparno Banyumas, 53122, Central Java, Indonesia.
[3]Departement of Health, Politeknik Negeri Nusa Utara. Jl. Kesehatan No 1, Kepulauan Sangihe 95812, North Sulawesi, Indonesia.
*Corresponding author: walter.balansa@fullbrightmail.com

Manuscript received: 29 Oct. 2025 Revision accepted: 12 Dec. 2025

Abstract

Marine biofouling causes significant economic and environmental damage creating an urgent demand for eco-friendly antifoulants. This *in silico* study aimed to evaluate the antifouling efficacy and ecotoxicological profile of macrolactin A (**1**), previously isolated from Indonesian sponge-associated *Bacillus* spp., alongside its computationally generated derivatives (**1a-1f, 2a–2k**) using Biotransformer 3.0. Molecular docking was utilized to assess binding affinities against key protein targets—the bacterial BAM complex, GSK-3β, and acetylcholinesterase (AChE)—and used EPI Suite™ to predict environmental safety. All tested compounds exhibited robust binding affinities (> -8.0 kcal/mol) against all targets likely binding to allosteric sites. ANOVA revealed significant differences ($p < 0.05$) in binding strength, with derivatives displaying a distinct preference for GSK-3β over AChE and BAM ($p < 0.01$). However, the broad-spectrum affinity across all three targets supports a potential multi-mechanism mode of action. Crucially, most derivatives showed low toxicity and bioaccumulation potential compared to commercial antifoulants such as Irgarol 1501, SeaNine 211, and Selektope®. Notably, analogues **1a-1c** and **2e** were predicted to be readily biodegradable. This study identified **1a–1c** and **2e** as leading candidates for eco-friendly antifoulants and provides a strong basis for future experimental development of novel, sustainable marine coating candidates.

Keywords: ecofriendly antifouling; in silico; macrolactin; molecular docking; sponge-associated bacteria

INTRODUCTION

Marine biofouling is a pervasive and costly problem that incurs 25 bilions of dollars in annual damages across fisheries and maritime industries globally (Olick, 2023). This undesirable accumulation of organisms on submerged surfaces destroys propeler, increases ship drag and gas emissions (Ayesu, 2023; Farkas, Degiuli, Martić, & Vujanović, 2021; S. Song, De Marco Muscat-Fenech, & Demirel, 2021), compromises structural integrity (Vedaprakash, Senthilkumar, Inbakandan, & Venkatesan, 2022), reduces aquaculture productivity (Bannister, Sievers, Bush, & Bloecher, 2019), and facilitates invasive species transfer (Georgiades et al., 2021; Yousef, 2023). While traditional antifouling coatings are effective, they are increasingly restricted due to the environmental harms caused by heavy metals and toxic biocides (Selim et al., 2017). Consequently, there is an urgent need for novel, effective, and environmentally benign strategies (Dobretsov & Rittschof, 2023).

Marine sponges and their symbiotic microorganisms offer unparalleled sources of novel bioactive compounds (J. A. Kim, Choi, Lim, & Kim, 2025; Sathiyanarayanan, Saibaba, Kiran, Yang, & Selvin, 2017). Our previous investigations into Sangihe sponge-symbiotic microorganisms (*Bacillus* sp.) yielded the known potent antimicrobial, antiviral, and anticancer 14-C surfactin and macrolactin A (Riyanti et al., 2020). We demonstrated both compounds exhibited antibacterial activity against MRSA, highlighting their potential efficacy against marine biofilm bacteria (Riyanti et al., 2020). Similarly, our earlier antifouling study on sarasinosides indicated that their antifouling activity might stem from their

http://ejournal.unsrat.ac.id/index.php/platax 10.35800/jipv10i2.65278

ability to interfere with the cholinergic system and their anticancer properties (Balansa, Riyanti, Rieuwpassa, & Hanif, 2025). Thus, we hypothesize that similar to potent antibacterial and anticancer compounds such as agelasines (Balansa et al., 2024; Balansa, Riyanti, Patras, et al., 2025) and bromopyrole alkaloids hymeniadesine and its debromo derivative (Qing et al., 2013), which are known antifouling agents, the antiviral, antimicrobial, and anticancer activities of macrolactin A may directly contribute to antifouling activity—a significant knowledge gap that requires urgent investigation.

This hypothesis aligns with the modern multi-pronged approach toward biofouling control, which targets both initial adhesion and the subsequent growth of biofilm-forming microorganisms (L Chen & Qian, 2017). Macrolactin A, a polyene macrolactone, exhibits a wide range of distinct biological activities—including antimicrobial, antiviral, and anticancer effects (Muhammad Abdul Mojid Mondol & Shin, 2014; Ortiz & Sansinenea, 2020) — that could complement the discovery of new antifoulants. For instance, a 2014 study showed that specific structural features, such as the position of the hydroxyl group (OH), the introduction of a keto group (C=O), or the addition of ester groups at C-7, dictate the antimicrobial potency of macrolactones (Muhammad Abdul Mojid Mondol & Shin, 2014). Similarly, the presence or absence of either hydroxyl or methoxyl at position 15 of the 24-membered lactone (Mohamad Abdul Mojid Mondol et al., 2013; Y. Song et al., 2024), whether they are cyclic or 22-membered lactones, and their geometric isomerism, all play a crucial role in the antimicrobial efficacy of macrolactins (Nagao, Adachi, Sakai, Nishijima, & Sanoll, 2001). Interestingly, while aglycon macrolactins were recently reported as potent anti-quorum sensing compounds, they did not show any antimicrobial actiivity (Y. Song et al., 2024). These findings underscore the importance of generating and evaluating various analogues of macrolactin A to rationally design sustainable coatings. However, the structural complexity and scarcity of macrolactin sources have long precluded drug development from this promising structural class (T. Wu, Xiao, & Li, 2021). These challenges, coupled with strict environmental constraints, necessitate the efficient design and affordable technological application of new solutions, moving beyond traditional, resource-intensive, and limited experimental approaches (Norouzi et al., 2025).

Computational methodologies, such as molecular docking and physicochemical predictions, offer a powerful and environmentally responsible alternative to traditional screening (Ma, Ajibade, & Zou, 2024; Norouzi et al., 2025). These methods allow for the rapid screening of compounds, prediction of molecular interactions, and elucidation of mechanisms, thereby reducing costly laboratory work. A crucial strategy involves integrating insights from controlled chemical modifications with complex biological and environmental transformations to identify novel, ecologically relevant derivatives for example through the use of computational tools such as Biotransformer 3.0 (Wishart et al., 2022) and EPI Suite™ (Card et al., 2017). These techniques can systematically generate diverse macrolactin A derivatives, allowing us to rapidly predict their antifouling potential and structural optimization for eco-friendly marine coatings.

Therefore, this study aims to develop a comprehensive in silico model to investigate multi-pronged antifouling of macrolactin A and derivatives for marine applications. Specifically, the study aims to: (1) predict the binding affinities of macrolactin A and its derivatives against acetylcholinesterase, GSK-3b and antimicrobial targets via molecular docking, (2) compare the different binding affinity against the three protein targets through ANOVA one way analysis and (3) characterize the key physicochemical characteristics of macrolactin A and its derivatives against commercial antifoulants. This in silico investigation provides a rational, environmentally

http://ejournal.unsrat.ac.id/index.php/platax 10.35800/jipv10i2.65278

conscious foundation for designing innovative, multi-functional marine coatings.

METHOD

Protein Preparation

The crystal structures of acetylcholinesterase (AChE; PDB ID: 6G1U) and glycogen synthase kinase-3β (GSK-3β; PDB ID: 1YPX) and BAM (5D0O) were retrieved from the Protein Data Bank (RCSB PDB). Each structure was prepared using Discovery Studio Visualizer: water molecules and heteroatoms were removed; polar hydrogens were added. The prepared proteins were imported into PyRx 0.9.9 as macromolecules for docking (Dallakyan & Olson, 2015).

Ligand Preparation

The structure of macrolactin A was adopted from our previous isolation study (Riyanti et al., 2020), where its identity was confirmed via spectroscopic data analysis (^{1}H, ^{13}C NMR and HRESIMS). It was drawn using ChemDraw Ultra 12.0, converted to a 2D structure, and saved as a .cdx file. The structures of analogues **2–7** were obtained by uploading the SMILES string of **1** to the BioTransformer 3.0 web server, with the metabolism predictor set to "Phase II" (conjugative reactions including sulfation and glucuronidation) as well as environmental and microbial biotransformation. This generated six metabolites (three per reaction type) for phase II and 11 for environmental and microbial biotransformation. Each metabolite SMILES was imported into ChemDraw Ultra 12.0, converted to 3D, and saved as .cdx files. All ligands (.cdx) were then imported into PyRx, minimized using the Open Babel module, and converted to pdbqt format.

Molecular Docking

Docking was performed using AutoDock Vina in PyRx with default parameters (exhaustiveness = 8). For AChE (6G1U), the grid box was centered at x = 65.6271, y =141.9604, z =111.6365 (dimensions: 20 × 20 × 20 Å). For GSK-3β (1Q5K), the grid box was centered at x = 71.3020, y = 77.1839, z = 99.1125 (dimensions: 20 × 20 × 20 Å). Nine binding modes per ligand were generated, and the lowest-energy pose (most negative binding affinity) was selected for analysis.

Biotransformation Analysis

Analogues **2–7** of macrolactin A were predicted using BioTransformer 3.0, a web-based tool for small-molecule metabolism prediction (Wishart et al., 2022). The SMILES string of macrolactin A (PubChem CID: 6442197) was uploaded, and the "Phase II" module was selected to simulate mammalian conjugative metabolism (glucuronidation and sulfation). This yielded six metabolites (**2–7**), with structures confirmed via SMILES output. Predicted metabolites were evaluated for antifouling potential against AChE, GSK-3β, and beta-barrel assembly machinery (BAM) via molecular docking.

Ecotoxicological Analysis

Ecotoxicological profiles were assessed using EPI Suite™ v4.11 (U.S. EPA), a QSAR-based toolkit for physicochemical and environmental fate predictions. SMILES strings of **1–7** were input to estimate key endpoints: octanol-water partition coefficient (Log Kow via KOWWIN™), organic carbon-water partition coefficient (Log Koc via KOCWIN™), bioconcentration factor/bioaccumulation factor (Log BCF/BAF via BCFBAF), and toxicities (Ames mutagenicity, hepatotoxicity, *Tetrahymena pyriformis* growth inhibition, and fathead minnow LC_{50} via ECOSAR™). A composite toxicology score was calculated per a published multi-endpoint method, weighting acute/chronic aquatic risks and biodegradation potential (BIOWIN™ for ready biodegradability) (Card et al., 2017).

Statistical Analysis

Binding affinities (kcal/mol) from molecular docking of macrolactin A (**1**), analogues 2–7, spongiacidins A and D, and their derivatives against AChE, GSK-3β, and BAM were compared using one-way ANOVA (single factor) in Microsoft Excel 365. This parametric test assessed differences among ligand means for each

http://ejournal.unsrat.ac.id/index.php/platax 10.35800/jipv10i2.65278

target, assuming normality (Shapiro-Wilk test, p > 0.05) and homoscedasticity (Levene's test, $p > 0.05$). Post-hoc Tukey's HSD test identified pairwise differences (α = 0.05). ANOVA evaluates the null hypothesis of equal group means via F-statistic, suitable for >2 groups. Data were reported as mean ± SD (n = 9 poses/ligand).

RESULTS AND DISCUSSION

Building upon our early discovery of C-14 surfactin and antibacterial macrolactin A (Riyanti et al., 2020), this study aimed to evaluated the unknown antifouling potential of macrolactin A and its derivatives (**1-7**) by targeting acetylcholinesterase, GSK-3b and BAM. The results confirmed the multi-pronged antifouling activity of the macrolactin A (**1**) and its derivatives (**1a-1f, 2a-2k**), showing strong interactions among all compounds and their protein targets mostly through allosteric binding. Moreover, computation prediction of their ecotoxicological profiles showed low toxicity, low bioaccumulation potential and fast biodegradation particularly for glucuronidated (**1a-1c**) and hydroxylated (**2c**) derivatives described in detail in this section.

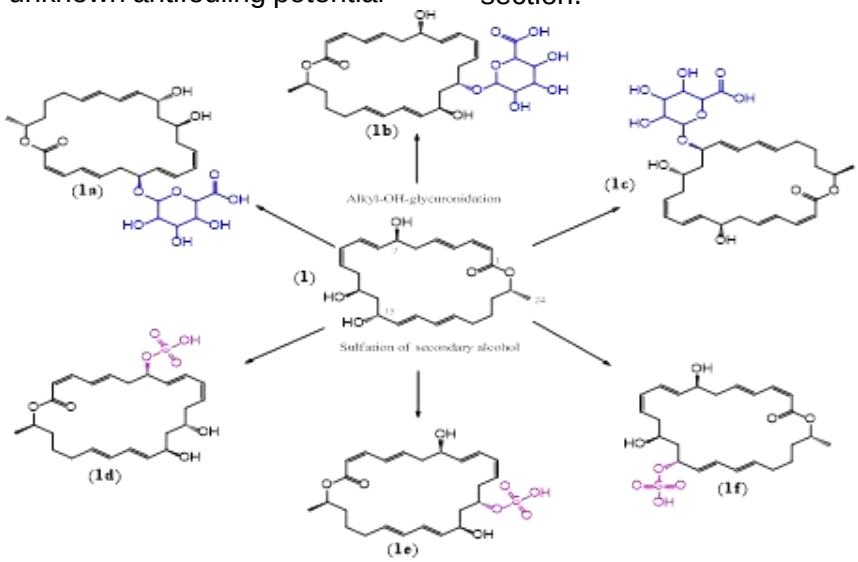

Figure 1. Biotransformation products of macrolactin A obtained through phase II biotransformation using Biotransformer 3.0, showing alkyl-OH-glucuronidation and sulfation of secondary alcohol.

The in-silico biotransformation analysis of macrolactin A (**1**) predicted the formation of six Phase II metabolic derivatives (**1a–1f**). Specifically, the analysis identified three *O*-glucuronidation products including macrolactin A 7-*O*-glucuronide (**1a**), 13-*O*-glucuronide (**1b**), and 15-*O*-glucuronide (**1c**). These analogues were formed via the attachment of a glucuronic acid moiety to the secondary alcohol groups at positions C-7, C-13, and C-15, respectively. Similarly, the computational model predicted three sulfated derivatives including macrolactin A 7-*O*-sulfate (**1d**), 13-*O*-sulfate (**1e**), and 15-*O*-sulfate (**1f**). This sulfation process involves the enzymatic transfer of a sulfate group (-OSO_3H) to the corresponding hydroxyl functionalities, a modification known to significantly alter physicochemical properties (Figure 1) (Coughtrie, 2016).

While prior biotransformation studies on agelasines and imidazoquinolinone have consistently demonstrated the dominance of glucuronidated metabolites over sulfated ones (Docampo-Palacios et al. 2020; Balansa, Rieuwpassa, and Hanif 2025; Balansa, Riyanti, Balansa, et al. 2025; Hinonaung et al. 2025), our in-silico analysis of macrolactin A (**1**) predicted a comparable prevalence of both conjugate types. This divergence is likely attributable to the inherent complexity of biological systems, which poses a significant challenge for scientists in creating accurate models (Puniya, 2025). The absence of

http://ejournal.unsrat.ac.id/index.php/platax 10.35800/jipv10i2.65278

direct measurement, coupled with noisy and incomplete data, often leads to imprecise estimations in such models (Puniya, 2025). Specifically, the software likely identified the macrolide's three secondary hydroxyl groups as equally viable nucleophilic acceptors for both glucuronic acid transferases (UGT) and sulfotransferases (SULT) enzymes. This contrasts with *in vivo* systems, where cofactor availability and enzyme capacity typically favor glucuronidation (Pan et al., 2021), unlike the software, which uniformly applies metabolic rules based solely on the molecule's topology. Consequently, the resulting symmetrical output reflects a qualitative inventory of chemically feasible transformations rather than the quantitative regioselectivity observed in biological settings. Furthermore, while previous research has explored macrolactin derivatives generated via type I polyketide synthases (PKS)—yielding epoxidized, glycosylated, and acylated products with improved bioactivity (T. Wu et al., 2021)—this study represents the first to specifically investigate the generation of glucuronidated and sulfated metabolites, alongside microbial and environmental biotransformation products, as potential antifouling candidates.

The biotransformation of macrolactin A by environmental and microbial processes generates dehydrogenated, hydroxylated, and hydrolytic cleavage products (Figure 2), potentially altering their bioactivities. Derivatives 7-, 13-, and 15-oxo-macrolactin A (**2a**, **2b**, **2e**) are likely produced via non-specific alcohol dehydrogenases, a process similar to enzymatic transformations in bacteria like *Clostridium* and *Eubacterium* (Fiorucci et al., 2021). These modifications can influence the molecule's interaction with ribosomal targets, as even subtle changes to the macrolactone ring are known to affect activity against pathogens like *Staphylococcus aureus* (Chadha, Padhi, Stella, Venkataraman, & Saravanan, 2024). Additionally, the formation of derivative **2c** is attributed to oxidative enzymes such as cytochrome P450 monooxygenases. These enzymes introduce hydroxyl groups, increasing polarity and potentially diversifying biological profiles, similar to how P450s modify macrolide antibiotics like pikromycin (Graziani, Cane, Betlach, Kealey, & McDaniel, 1998). Finally, a linear product (**2g**) is formed by microbial esterases or environmental hydrolysis. This lactone ring cleavage, which is also observed in macrolide antibiotic resistance (e.g., via erythromycin esterases), abolishes the conformational rigidity critical for macrolactin A's biological activity against targets like *Bacillus subtilis* (Zieliński, Park, Sleno, & Berghuis, 2021).

The biotransformation of macrolactin A also involves significant modifications to its conjugated polyene system, a structural feature critical for both its biological activity and physicochemical properties. Derivatives such as **2f** and **2h**–**2k** exemplify the saturation of specific carbon-carbon double bonds across the macrocyclic ring through enzymatic reduction. This process implies the activity of alkene reductases (Sun, Van Loey, Buvé, & Michiels, 2023), which regioselectively reduce the diene or triene motifs within the macrolactin A structure (Figure 2). These reductive steps may disrupt the bioactivity of macrolactin A because the number of conjugated double bonds on the macrolactone ring dictate their rigidity, hydrophobicity, and stability of the bioactivity of thier antibacterial, the antifungal activity and toxicity (Qiao, Dong, Zhou, & Cui, 2023). Collectively, the generation of these saturated analogs suggests that environmental microbes may utilize reductive pathways as a mechanism to detoxify the polyene antibiotic.

Traditionally, biotransformation pathways are viewed as detoxification mechanisms that increase hydrophilicity to facilitate excretion (Gagan & et al., 2012) and deactivate metabolites (Järvinen et al., 2022; Tornio et al., 2014). However, biotransformed products—whether resulting from environmental degradation or microbial metabolism—are increasingly recognized for their potential to possess improved biological activity (Balansa, Riyanti, Balansa, et al., 2025; Balansa et al., 2024). These structural modifications fundamentally increase hydrophilicity,

http://ejournal.unsrat.ac.id/index.php/platax 10.35800/jipv10i2.65278

which profoundly impacts bioavailability, distribution, and ecotoxicological profiles (Docampo-Palacios et al., 2020; Escher & Schwarzenbach, 2002). Consequently, evaluating these derivatives via molecular docking and EPI Suite™ is crucial for early-stage prediction of both efficacy and safety in eco-friendly antifouling discovery.

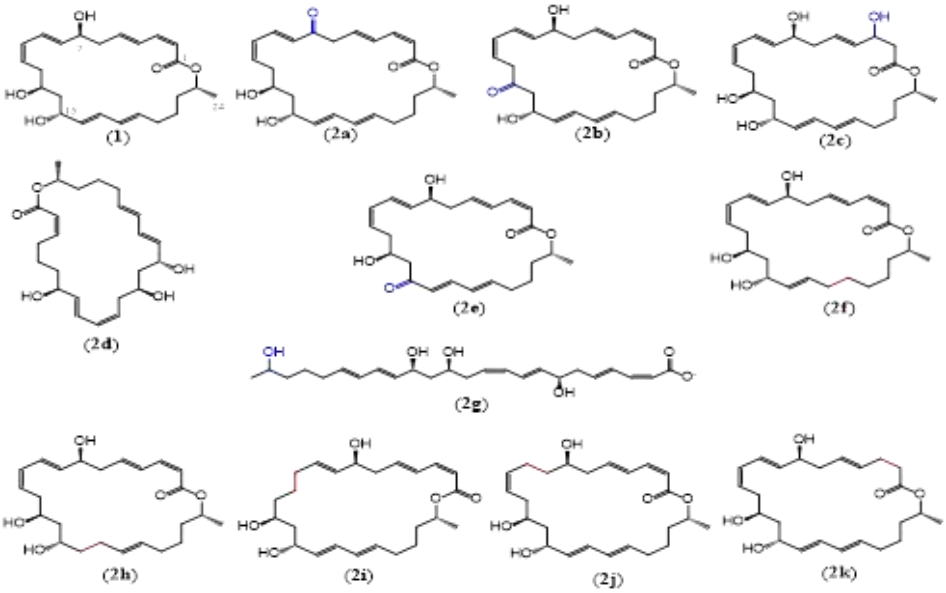

Figure 2. Biotransformation products of macrolactin A obtained through Environmental and Microbial Biotransformation using Biotransformer 3.0, showing dehydrogenated, hydroxylated metabolites.

Molecular docking analysis of macrolactin A (**1**) and its derivatives (**1a**-**1f**, **2a**-**2k**) revealed strong binding affinities against Glycogen Synthase Kinase-3 beta (GSK-3β, PDB ID: 1PYX), acetylcholinesterase (AChE, PDB ID: 6G1U), and the Beta-barrel Assembly Machinery (BAM, PDB ID: 5D0O) (Table 1, Figure 2). Macrolactin A and its analogues consistently exhibited binding energies lower (i.e., stronger) than -8.0 kcal/mol. Notably, while most derivatives—with the exception of the linear product **2g**—showed improved binding affinity against GSK-3β compared to the parent molecule, fewer derivatives matched the parent molecule's potency against acetylcholinesterase and BAM (Table 1).

Comparative molecular docking analysis reveals a distinct selectivity for macrolactin A and its derivatives (**1a–2k**), with the scaffold generally exhibiting the highest affinity for Glycogen Synthase Kinase-3 beta (GSK-3β, PDB ID: 1PYX). As illustrated in Figure 3, a significant proportion of the derivatives, particularly **1d**, **2a**, and **2e** with binding affinities of -11.33±0.78, -10.87±0.12 and -10.83±0.15 Kcal/mol respectively surpassed the high-affinity threshold of -10.0 kcal/mol against GSK-3β, suggesting a favorable interaction fit for the kinase binding pocket. In contrast, binding energies for Beta-barrel Assembly Machinery (BAM, PDB ID: 5D0O) and acetylcholinesterase (AChE, PDB ID: 6G1U) were generally more moderate, predominantly clustering between -8.0 and -9.5 kcal/mol. A notable exception to these trends is derivative **2g**, which displayed a marked reduction in binding affinity across all three targets (energies > -8.0 kcal/mol); this loss of potency corroborates the hypothesis that the conformational rigidity provided by the intact lactone ring is a critical determinant for effective ligand-protein interaction (Ortiz & Sansinenea, 2020; Xu et al., 2024). Overall, while the macrolactin scaffold demonstrates broad-spectrum potential, the data highlights a specific structural preference for GSK-3β inhibition over neuro-enzymatic targets.

http://ejournal.unsrat.ac.id/index.php/platax 10.35800/jipv10i2.65278

Table 1. Binding affinities of macrolactin A (**1**) and its derivatives (**1a-1f, 2a-2k**) against IPYX, 6G1U and 5D0O

Molecules	Binding affinity		
	IPYX (GSK-3b)	6G1U (AChE)	5D0O (BAM)
1a	-10.10±0.17	-8.70±0.22	-9.16±0.59
1b	-10.30±1.13	-9.20±0.20	-9.04±0.05
1c	-10.53±0.55	-9.00±0.37	-8.84±0.57
1d	-11.33±0.78	-8.88±0.36	-8.92±0.26
1e	-10.50±0.36	-8.24±0.57	-8.60±0.64
1f	-10.07±0.12	-8.92±0.40	-8.50±0.44
1g	-10.00±0.44	-8.42±0.33	-8.86±0.72
2a	-10.87±0.12	-8.70±0.30	-9.70±0.44
2b	-10.87±0.12	-8.60±0.19	-9.50±0.11
2c	-10.27±0.40	-8.30±0.12	-8.80±0.32
2d	-10.20±0.00	-8.60±0.31	-9.30±0.62
2e	-10.83±0.15	-8.50±0.15	-9.78±0.28
2f	-10.17±0.92	-8.60±0.20	-8.95±0.31
2g	-7.33±0.12	-7.80±0.23	-6.30±0.23
2h	-10.67±0.06	-8.30±0.05	-9.43±0.04
2i	-10.67±0.23	-8.60±0.49	-9.13±0.04
2j	-10.67±0.06	-8.70±0.41	-9.28±0.33
2k	-10.40±0.20	-8.40±0.21	-9.33±0.07
SB_216763	-8.70±0.12	NA	NA
Darobactin	NA	NA	-12.10
Tacrine	NA	-9.7±0.15	NA

The robust binding profile observed across these diverse target proteins suggests the potential of macrolactin A and its derivatives to support a multi-pronged antifouling strategy. This hypothesis is supported by the distinct physiological roles of the docked targets: inhibition of GSK-3β and AChE is known to disrupt eukaryotic larval settlement (T. H. Kim & et al., 2014) and cause neurobehavioral interference in fouling invertebrates (Rittschof, 2001), respectively, while targeting BAM prevents bacterial biofilm formation by hindering outer membrane protein assembly (Gumbart & et al., 2019). These strong binding characteristics—with energies consistently exceeding -8.0 kcal/mol and reaching as low as -11.0 kcal/mol—corroborate previous reports highlighting macrolactin A's inhibitory effect on SARS-CoV-2 Mpro and its role in inhibiting bacterial protein biosynthesis. This alignment with established literature further underscores the molecule's broad-spectrum biological activity and versatile scaffold (Jaramillo & et al., 2021; Zuo & et al., 2023).

Further structural analysis of the molecular docking results provided insight into the specific binding modes of the macrolactin derivatives within the *E. coli* BAM complex (Figure 4). While the majority of ligands interacted primarily with BamA—the central component of the BAM machinery—distinct binding profiles were observed for specific derivatives. For instance, compound **1c** targeted the regulatory subunit BamE, whereas compound **1d** exhibited a unique interaction pattern. Notably, compound **1d** bound to a site on BamA highly analogous to that of darobactin (DRB), a known potent BAM inhibitor that bind to the active site of this receptor (Kaur et al., 2021). Although **1d** displayed a slightly weaker binding affinity than darobactin, the overlap in binding location suggests that it may exploit a comparable inhibitory mechanism to disrupt outer membrane protein assembly. This contrasts with other derivatives, such as **1c**, which target peripheral subunits like BamE. This diversity in binding sites highlights that the biotransformation of macrolactin A

http://ejournal.unsrat.ac.id/index.php/platax 10.35800/jipv10i2.65278

generates analogues capable of targeting different structural vulnerabilities within the bacterial assembly machinery.

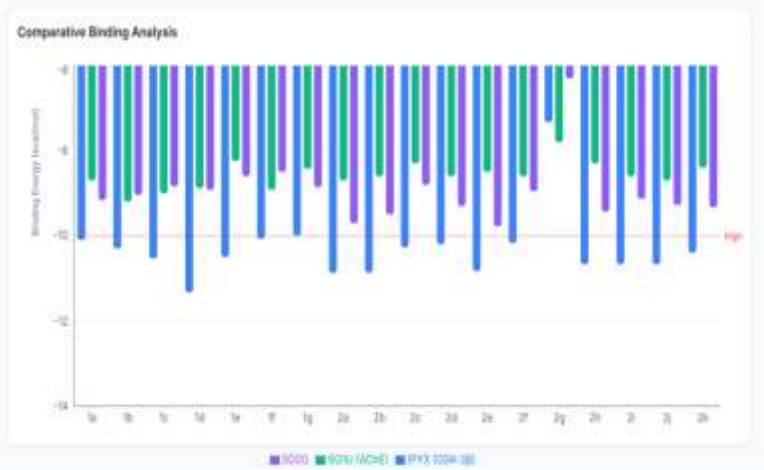

Figure 3. Binding analysis of macrolactin A's derivatives against BAM (PDB ID: 5D0O), acetylcholinesterase (PDB ID: 6G1U), and GSK-3β (PDB ID: 1PYX). While the highest bars represent the weakest binding, the lowest bars indicate the strongest binding affinity. The majority of the ligands show stronger binding affinity towards 1PYX (red bars) than 6G1U (purple bars) and 5D0O (green bars).

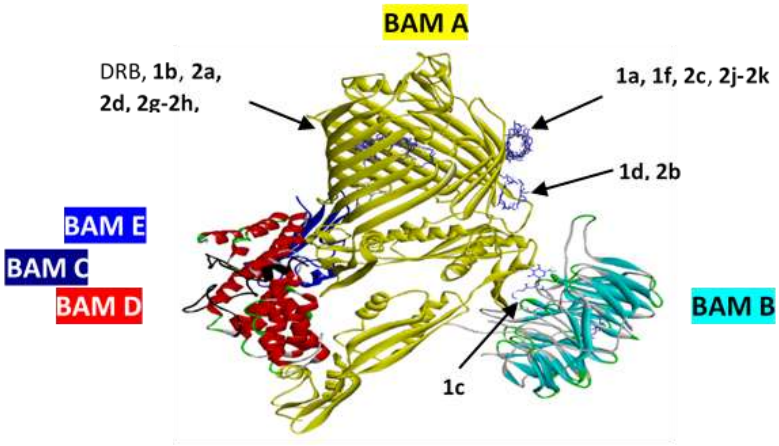

Figure 4. The structure of BAM complex of *E. coli*, showing BAM A (yellow), BAM B (cyan), BAM C (black), BAM D (red) and BAM E (blue) (Gu et al., 2016) and binding sites of macrolactin A (**1**) its derivatives (**1a-1f, 2a-2k**) and dorabaction (DRB) on the complex.

Moreover, molecular docking was conducted on acetylcholinesterease (AChE), which has an active site known as a long gorge approximately 20 Å in length. This gorge comprises a catalytic active site (CAS) at the bottom and a peripheral anionic site (PAS) near the entrancewith (Hung et al., 2025). Responsible for hydrolising AChE, the CAS forms the catalytic triad consiting of three amino acid residues Ser200, Glu327 and His440 while PAS consists o several aromatic residues including Tyr70, Tyr121 and Trp279. The resuls showed that all macrolactin ligands occupy a binding pocket distinct from that of tacrine, a potent reference inhibitor of acetylcholinesterase (W. Y. Wu et al., 2017). While tacrine is known to act as a dual-site inhibitor—spanning both the catalytic active site (CAS) and the peripheral anionic site (PAS) (Sameem et al., 2017)—the macrolactin derivatives exhibited a fundamentally different interaction profile (Figure 5).

http://ejournal.unsrat.ac.id/index.php/platax 10.35800/jipv10i2.65278

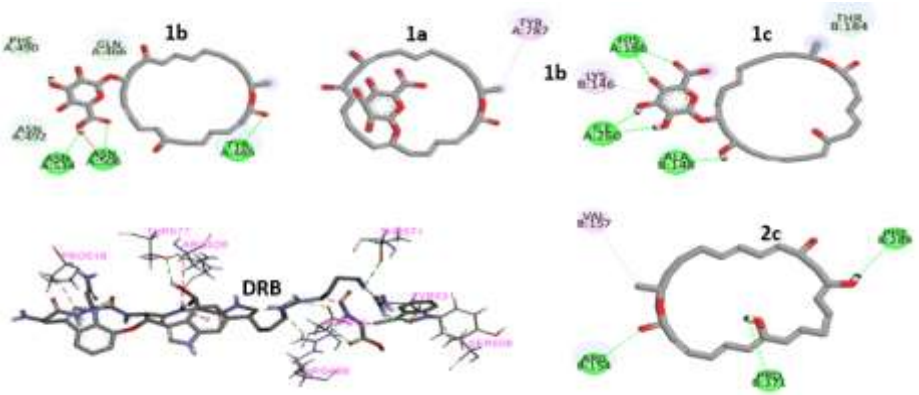

Figure 5. The binding of glucuronidated derivatives (**1b,1c)** on different sites of BAM A and and hydroxylated derivative (**2c**) on BAM E, showing distinct amino acid residues binding to different derivatives with hydrogen bonding (green), pink and green lines indicate hydrogen bonding.

This distinction is evidenced by the specific amino acid residues involved: tacrine showed characteristic interactions with Trp84, Tyr334, and Phe330, residues that define the active site gorge (Luque & Muñoz-Torrero, 2023). In contrast, macrolactin A and its derivatives (e.g., **1c**, **1d**) did not engage these key catalytic or gorge residues. This lack of overlap with the canonical tacrine binding site suggests that the macrolactin derivatives likely function through an allosteric mechanism, binding to a non-catalytic region of the enzyme to modulate its activity. Finaly, molecular docking on GSK-3 βrevealed distinct binding preferences among the macrolactin A derivatives. Similar to the parent compound, the 2-series metabolites (**2a–2k**) primarily occupy the region flanking the C- and N-terminal lobes (designated as Side A, red circle). In contrast, the 1-series (**1a–1f**, with the exception of **1c**) preferentially reside in a distinct region designated as the active site Side B (black circle) (Figure 6).

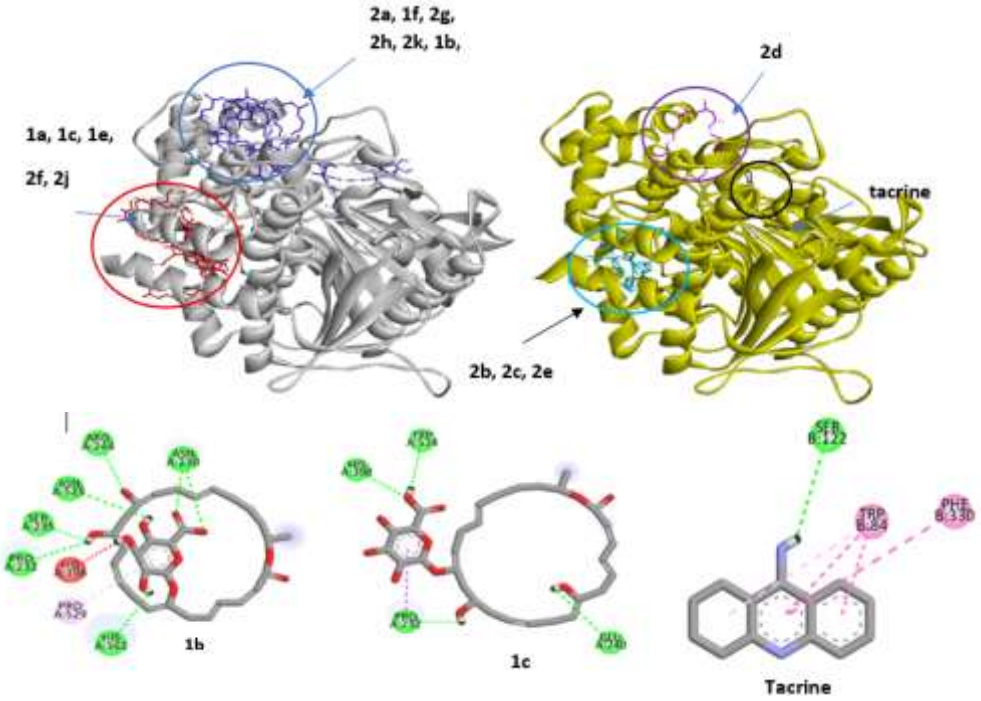

Figure 6. The structure of acetylcholinesterease (AChE), different binding sites of macrolactin A derivatives and amino acid redisues of 1b, 1c and tacrine showing distinct amino acid residues hydrogen bond (green), p-alkyl (pink), red (unfavourable bond)

http://ejournal.unsrat.ac.id/index.php/platax 10.35800/jipv10i2.65278

Finally, molecular docking on GSK-3 *β*revealed distinct binding preferences among the macrolactin A derivatives. Similar to the parent compound, the 2-series metabolites (**2a–2k**) primarily occupy the region flanking the C- and *N*-terminal lobes (designated as Side A, red circle). In contrast, the 1-series (**1a–1f**, with the exception of **1c**) preferentially reside in a distinct region designated as the active site Side B (black circle) (Figure 7). To validate these observations, the native ATP analog, AMP-PNP (ANP), was docked onto the enzyme. AMP-PNP bound to Side B, partially superimposing with the 1-series derivatives. Since AMP-PNP targets the ATP-binding pocket (Dixon-Clarke, Elkins, Cheng, Morin, & Bullock, 2015), this suggests that select 1-series molecules (e.g., **1c**) bind proximal to the active site. Conversely, the 2-series compounds (e.g., **2c**) docked near the binding site of SB216763, a known potent GSK-3*β* inhibitor located at Side A (Lee et al., 2022). Ultimately, the docking analysis suggests that both 1- and 2-series metabolites likely bind to allosteric sites rather than the catalytic core. This hypothesis is supported by the limited number of shared interacting residues, specifically Asp200 and Asp181 (shared between the 1-series and AMP-PNP) and Asp200 (shared between the 2-series and SB216763) (Figure 7).

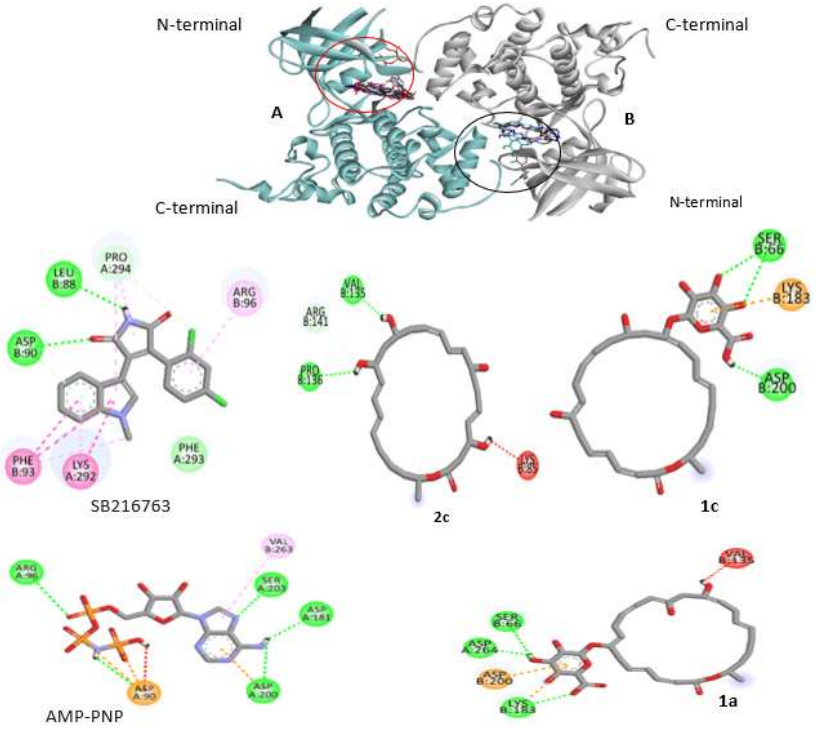

Figure 7. Structure of GSK-3b (PDB ID: 1YPX) and binding of macrolactin derivative (**1a-1f, 2a-2k**) and tacrin on the receptor showing most derivatives side A of the the GSK-3b recepor

To assess the overall differences in mean binding affinities among the three protein targets, an ANOVA single factor analysis was performed. The analysis yielded an F-statistic of 33.44 and a *p*-value of 0.00000000526. Comparing these values to the F critical value of 3.17 (at a standard significance level of α = 0.05), it is evident that the observed F-statistic is significantly higher than the F critical value, and the *p*-value is very significantly smaller than 0.05 (Table 2).

Statistical analysis (ANOVA single factor) revealed significant differences in the mean binding affinities of macrolactin A and its derivatives across the three protein targets: GSK-3*β* (PDB: 1PYX), Acetylcholinesterase (PDB: 6G1U), and the BAM complex (PDB: 5D0O) (Table 3). To determine the specific nature of these

http://ejournal.unsrat.ac.id/index.php/platax 10.35800/jipv10i2.65278

differences, a post-hoc analysis was performed using Welch's t-test (two-sample assuming unequal variances). To control for family-wise error rates across the three pairwise comparisons, a Bonferroni adjustment was applied, establishing a significance threshold of $\alpha = 0.017$ $(0.05/3)$ (Armstrong, 2014).

Table 2. Anova Single Factor

Groups	Count	Sum	Average	Variance
1PYX	18	-185.78	-10.32111111	0.678163399
6G1U	18	-154.46	-8.581111111	0.10331634
5D0O	18	-161.42	-8.967777778	0.566477124

Table 3. ANOVA

Source of Variation	SS	df	MS	F	p-value	F crit
Between Groups	30.05173333	2	15.02586667	33.44142624	5.26076E10	3.178799292
Within Groups	22.91526667	51	0.449318954			
Total	52.967	53				

Table 4. T-Test: Two-sample assuming unequal variances

	IPYX (GSK-3b)	6G1U (AChE)	5D0O (BAM)	IPYX (GSK-3b)	6G1U (AChE)	5D0O (BAM)
Mean	10.32111111	8.58111111	8.96777777	10.3211111	8.58111111	8.96777777
Variance	0.678163399	0.10331634	0.566477124	0.678163399	0.10331634	0.566477124
Observations	18	18	18	18	18	18
Hypothesized Mean Difference	0		0		0	
df	22		34		23	
t Stat	-8.350772254		5.146583972		2.004483725	
P(T<=t) one-tail	1.43715E-08		5.54342E-06		0.028464958	
t Critical one-tail	1.717144374		1.690924255		1.713871528	
P(T<=t) two-tail	0.0000000287		0.00001109		0.056929915	
t Critical two-tail	2.073873068		2.032244509		2.06865761	

The analysis demonstrated a statistically significant preference for GSK-3β compared to both Acetylcholinesterase ($p = 2.87 \times 10^{-7}$) and the BAM complex ($p = 1.11 \times 10^{-6}$) or p < 0.01 (Table 4). Conversely, the difference in binding affinity between Acetylcholinesterase and the BAM complex was not statistically significant ($p = 0.057$) or p > 0.01 (Table 4). These findings indicate that while the derivatives exhibit a distinct, statistically significant bias toward GSK-3β, they maintain substantial binding potential against the other targets. Despite the statistical preference for one pathway, the overall binding profile remains broad. This suggests that any variations in affinity for specific molecules are not merely artifacts of experimental variability, but rather reflect a nuanced interaction profile where the compounds favor GSK-3β while sufficiently engaging Acetylcholinesterase and BAM. Consequently, this multi-target interaction capability is advantageous for an antifouling strategy, as the compounds can simultaneously disrupt diverse biological mechanisms responsible for both bacterial and eukaryotic fouling without being strictly limited to a single pathway (P. Y. Qian, Chen, & Xu, 2013).

In-silico toxicity assessment using EPI Suite™ reveals that structural modifications resulted in varying

http://ejournal.unsrat.ac.id/index.php/platax 10.35800/jipv10i2.65278

ecotoxicological profiles among the lipophilic derivatives. The parent compound (**1**) exhibits moderate acute toxicity, with lethal concentrations (LC_{50}) ranging from 17.47 to 27.55 mg/L for daphnids and fish, respectively. In contrast, derivative **2g** displayed a less favorable profile; the cleavage of the lactone moiety in this analogue caused an increase in toxicity (e.g., lower LC_{50} and EC_{50} values against fish, daphnids, and green algae), predicted bioaccumulation (Log K_{ow} > 3.50), and persistence (Table 1). Conversely, while lipophilic derivatives **2a**, **2d**, and **2f-2k** retained toxicity profiles similar to the parent molecule, analogues **2b**, **2c**, and **2e** showed considerable improvement compared to macrolactin A. These specific analogues exhibited lower toxicity towards non-target organisms and were predicted to be non-bioaccumulative (Log K_{ow} < 3.5). Interestingly, the ketone derivatives **2a, 2b**, and **2e** share virtually the same structure—differing only by the ketone position on the 24-lactone ring (C7 for **2a**, versus C14 for **2b**)—yet displayed significantly different toxicity profiles.

In contrast, the hydrophilic derivatives (**1a–1f**) demonstrate a dramatic reduction in toxicity. For instance, derivative **1d** displays a 96-hour LC_{50} of 4242 mg/L for fish and 2167 mg/L for daphnids, representing a greater than 100-fold increase in safety margins compared to the parent molecule (Table 5). This trend correlates strongly with increased water solubility (e.g., 172.6 mg/mL for **1d** versus 5.5 mg/mL for **1**), suggesting that the introduction of polar groups limits the molecule's capacity to passively diffuse across biological membranes, thereby mitigating acute toxic effects. However, the environmental fate differs between the subclasses. Only the glucuronidated analogues (**1a–1c**) are predicted to biodegrade rapidly, whereas the sulfated analogues (**1d–1f**) are predicted to persist. Additionally, the benefit of the increased LC_{50} (4242 mg/L) in sulfated analogues is offset by a significant increase in EC_{50} (1042 mg/L). Consequently, despite an improved therapeutic ratio of approximately 4, significantly higher concentrations of these derivatives are required to achieve antifouling effects. This reduced potency, coupled with their predicted environmental persistence, identifies **1a–1c** as the most environmentally favorable candidates within the **1**-series.

Moreover, the physicochemical properties governing environmental fate indicate the suitability of specific lipophilic and hydrophilic derivatives as eco-friendly antifouling candidates. Macrolactin A (**1**) possesses an octanol-water partition coefficient (Log K_{ow}) of 3.20, placing it near the bioaccumulation threshold (ECHA 2017). However, the hydrophilic derivatives **1a–1f** exhibit significantly lower Log K_{ow} values (0.43 to 2.04), corresponding to negligible bioaccumulation potential (Log BCF/BAF < 1.0). This suggests that these compounds are unlikely to biomagnify in marine food webs (ECHA 2017). Additionally, despite their increased water solubility compared to the parent compound, derivatives **1a-1c** are considered to have moderate water solubility. This moderate solubility suggests better binding to the hydrophobic matrix of marine coatings and sustained release into the marine environment, particularly compared to derivatives **1d-1f** (Vilas Boas et al., 2021; Vilas Boas et al., 2023). Except for analogues **1d–1f** and **2g**, the parent compound and the remaining derivatives (**1a–1c** and **2a–2f**) are predicted to be rapidly biodegradable (Table 4). Notably, the linear derivative **2g** represents the most unfavorable environmental profile, featuring high lipophilicity (Log K_{ow} 3.85), high toxicity, and predicted persistence. In contrast, the introduction of an extra hydroxyl group in **2c** significantly increased its LC_{50} (444.15 mg/L) by approximately 16-fold and its EC_{50} (177.34 mg/L) by approximately 5.6-fold compared to macrolactin A (Table 5). Although this derivative slightly loses antifouling effectiveness, it becomes significantly less toxic than macrolactin A.

Although compounds **1a–1c** and **2c** (along with **2e**) may display a smaller therapeutic ratio LC_{50}/EC_{50} (2.32 for **1a-1c** to 2.50 for **2c** vs.4.6, 6.6 and >200 for Selektope, Seanine 211 and Irgarol

http://ejournal.unsrat.ac.id/index.php/platax 10.35800/jipv10i2.65278

respectively) compared to potent commercial agents like SeaNine 211, Irgarol 1501, and Selektope, they represent a superior environmental alternative due to their favorable eco-profiles. Unlike the commercial antifoulants, which are characterized by a lack of biodegradability and high soil adsorption (Log Koc > 2.85, Log Kow >3.5 for irgarol 1501 and SeaNine 211), leading to persistent sediment accumulation, the proposed ligands demonstrate fast biodegradation and significantly lower Koc win values (e.g., 0.214 for **1a–1c**). This combination of rapid breakdown and low sorption potential ensures that **1a–1c** and **2c** do not bioaccumulate in marine ecosystems, making them safer, non-persistent candidates despite the trade-offs in their therapeutic ratios.

Table 5. Toxicity data of **1a-1fm 2a-2k** (EPI Suite^{TM})

Ligands	Water solubility mg/mL	Fish 96 hr LC_{50} mg/L	Daphnid 48 hr LC_{50} mg/L	Green Algae 96 hr EC_{50}	Log K_{ow} L/kg ww	Log BCF L/kg ww	Log BAF L/kg ww	BHL	K_{oc} win/Log Koc	Fast Biodegradation
1	5.45	27.55	17.47	20.59	3.200	1.78	1.88	0.04	1.807	Yes
1a	10.03	440.44	250.94	189.58	2.037	0.50	0.93	0.04	0.214	Yes
1b	10.03	440.44	250.94	189.58	2.037	0.50	0.93	0.04	0.214	Yes
1c	10.03	440.44	250.94	189.58	2.037	0.50	0.93	0.09	0.214	Yes
1d	172.60	4242.13	2166.81	1042.03	0.854	0.50	0.14	0.05	0.668	No
1e	172.60	4242.13	2166.81	1042.03	0.854	0.50	0.14	0.05	0.668	No
1f	172.60	4242.13	2166.81	1042.03	0.854	0.50	0.14	0.05	0.668	No
2a	8.68	43.45	27.00	29.32	2.975	1.63	1.67	0.21	1.880	Yes
2b	15.32	78.18	47.76	46.35	2.690	1.44	1.47	0.17	1.720	Yes
2c	56.75	444.15	249.83	177.34	1.878	0.91	0.79	0.08	1.076	Yes
2d	3.467	17.74	11.48	14.46	3.416	1.92	0.38	0.38	1.920	Yes
2e	8.685	43.49	27.00	29.23	2.979	1.63	1.67	0.21	1.880	Yes
2f	3.467	17.74	11.48	14.46	3.416	1.92	0.38	0.38	1.920	Yes
2g	2.895	7.46	5.03	7.60	3.850	0.50	2.07	0.32	1.460	No
2h	3.467	17.74	11.48	14.46	3.416	1.92	0.38	0.38	1.920	Yes
2i	3.467	17.74	11.48	14.46	3.416	1.92	0.38	0.38	1.920	Yes
2j	3.467	17.74	11.48	14.46	3.416	1.92	0.38	0.38	1.920	Yes
2k	3.467	17.74	11.48	14.46	3.416	1.92	0.38	0.38	1.920	Yes
SeaNine 211	14.000	0.02	0.005	0.003	4.650	2.85	3.20	0.01	3.360	No
Irgarol 1501	7.000	1.300	11.60	0.006	3.950	2.40	2.10	0.05	3.280	No
Selektope®	185.00	85.200	42.50	18.500	2.910	1.45	1.10	0.20	2.850	No

Collectively, these data indicate a clear divergence in safety profiles. While the hydrophilic derivatives (**1a–1f**) generally show reduced toxicity, the glucuronidated analogues (**1a–1c**) are superior to their sulfated counterparts (**1d–1f)** due to their rapid biodegradability. Similarly, among the lipophilic series, analogues **2c** showed considerably more favorable ecotoxicological profiles than other 2-series. This sensitivity to regiochemistry indicates that the macrolactin scaffold is amenable to structural fine-tuning, a feature that is particularly advantageous for the discovery of environmentally benign antifouling agents.

This in silico study leveraged computational methodologies to explore the potential of macrolactin A derivatives as antifouling candidates. The physicochemical properties governing environmental fate are crucial for evaluating eco-friendly antifouling agents.

http://ejournal.unsrat.ac.id/index.php/platax 10.35800/jipv10i2.65278

Specifically, macrolactin A (**1**) possesses an octanol-water partition coefficient (Log K_{ow}) of 3.20, which places it near the bioaccumulation threshold (ECHA 2017). In contrast, its hydrophilic derivatives (**1a–1f**) exhibit significantly lower Log Kow values (0.43 to 2.04), corresponding to negligible bioaccumulation potential (Log BCF/BAF < 1.0). Molecular docking analysis revealed that macrolactin A (**1**) and its derivatives (**1a**–**1f**, **2a**-**2k** excluding **2g**) consistently demonstrated robust binding affinities (ranging from -8.24 to -11.56 kcal/mol) against three crucial protein targets: GSK-3β (PDB: 1PYX), AChE (PDB: 6G1U), and BAM (PDB: 5D0O). This broad-spectrum binding profile suggests a multi-pronged antifouling mechanism capable of simultaneously interfering with diverse biological pathways underpinning biofouling. Furthermore, single-factor ANOVA analysis demonstrated a statistically significant difference in mean binding affinities across these targets, indicating that while these derivatives function as multi-target inhibitors, they exhibit a distinct preferential affinity for GSK-3β over AChE and BAM.

These findings align with the known structural diversity and myriad biological activities of macrolactin A, including antibacterial, antiviral, anti-inflammatory, and other relevant bioactivities (Xu et al., 2024). Notably, this study is the first to report macrolactin A's anticancer activity within the context of antifouling potential, suggesting these combined activities likely contribute to their observed efficacy. Additionally, while previous studies have acknowledged the importance of both hydroxyl and methoxyl groups for the antimicrobial activity of macrolactins, this research shows that replacing either the hydroxyl group with glucuronic acid or modifying the double bond adjacent to lactone A slightly reduces antifouling effectiveness (indicated by an increased EC_{50}) but significantly improves ecotoxicological parameters (indicated by an increased LC_{50}).

Crucially, this *in-silico* ecotoxicological assessment using EPI Suite™ predicted improvement in the environmental profiles of a few derivatives. For instance, analogues **1a–1c** and **2c** exhibited favorable characteristics such as (1) robust binding affinity (>8.5 kcal/mol) against the studied protein targets, (2) reduced acute toxicity to aquatic organisms (fish, daphnids, and green algae), and (3) lower bioconcentration potential, evidenced by reduced Log K_{ow}, BCF, and BAF values (Table 4). Moreover, these derivatives are predicted to biodegrade rapidly, potentially mitigating concerns regarding environmental accumulation. While derivatives **1d–1f** also showed improved toxicity profiles, their predicted slow biodegradation rates and significantly increased EC_{50} (1042.03 mg/L) suggest they require further structural optimization before they can be considered environmentally benign.

The necessity for such optimization stems from the limitations of conventional screening protocols, which typically prioritize extreme lethality (low EC_{50} values). As evidenced by current commercial standards, this high potency often correlates with detrimental environmental characteristics. For instance, while Seanin and Irgarol exhibit exceptional potency ($EC_{50} \leq 0.006$ mg/L), they are plagued by environmental persistence (classified as non-biodegradable) and high bioaccumulation potential (Log BCF ranges from 2.40 to 2.85, Low K_{ow} > 3.5 particularly for Irgarol and Seanin) (Table 4). Not surprisingly, the accumulation of agents such as Seanin, Irgarol, and Selektope has been increasingly reported as a threat to marine ecosystems (Cai, Apell, Pflug, McNeill, & Bollmann, 2021; Lianguo Chen & Qian, 2017; Nyström et al., 2002; Ohji, Harino, Hayashizaki, Yusoff, & Inoue, 2023). Consequently, this study shifted the selection paradigm to prioritize environmental fate parameters—specifically biodegradability, bioaccumulation factor (BCF), and the therapeutic ratio (TR)—over raw biocidal power.

Under this "eco-friendly" screening framework, the synthesized ligands were stratified into two distinct categories. The

http://ejournal.unsrat.ac.id/index.php/platax 10.35800/jipv10i2.65278

first group comprises potent but toxic candidates (compounds **2a–2k**, excluding **2c**). While these derivatives displayed higher potency (EC_{50} 14–46 mg/L), they failed the safety assessment; their toxicity to non-target organisms (LC_{50}) tracked too closely with their effective concentrations, resulting in a therapeutic ratio (LC_{50}/EC_{50}) approaching unity ($TR \approx 1$). This narrow safety window renders them ecologically hazardous (P.-Y. Qian, Xu, & Fusetani, 2010; Wang, Wu, Wang, Wang, & Xu, 2017). In contrast, the eco-friendly candidates (**1a–1c** & **2c**) demonstrated a superior environmental profile characterized by rapid biodegradability ("Yes") and negligible bioaccumulation (Log BCF 0.50–0.91). This represents a significant improvement over commercial controls, which are predicted to persist in the environment and accumulate in aquatic tissues (Table 4).

Therefore, compounds **1a–1c** and **2c** were identified as the most promising antifouling candidates in this study. Despite their lower absolute potency—evidenced by the increase in EC_{50} (e.g., 189.58 mg/L for **1a**)—they offer a substantial increase in the fish survival threshold (LC_{50} = 440.44 mg/L). This selection represents a deliberate strategic trade-off: sacrificing the extreme lethality of commercial biocides to achieve biodegradable analogues that avoid the critical persistence and bioaccumulation issues associated with the commercial antifoulants.

Although computational models provide a theoretical framework rather than empirical proof, they serve as an essential basis for prioritization. This approach aligns with the modern search for new antifoulants, which requires molecules capable of modulating the complex pathways of the biofouling process. This concept is supported by Chen et al. (2023; 2024) , who argued that biofouling mitigation depends on the synergistic effects of multiple mechanisms rather than single-target actions. This paradigm favors candidates like macrolactin A, which possesses diverse molecular activities and multi-target potential (Jiamin Chen et al., 2019). Consequently, future research should focus on the targeted synthesis of the identified promising macrolactin A derivatives—adapting established protocols such as those for malonyl macrolactin A (Guglya et al., 2025; Onuh, Manopaek, Vangnai, Tiyayon, & Vinayavekhin, 2025)—followed by experimental validation in vitro and in field studies. Specifically, assays against the identified molecular targets and toxicity screenings on non-target marine organisms are warranted to confirm their potential as next-generation, environmentally benign antifouling agents.

CONCLUSIONS AND SUGGESTIONS

Conclusion

To conclude, this *in silico* study successfully mapped the metabolic and environmental biotransformation landscape of macrolactin A, identifying the glucuronidated **1a–1c** and hydroxylated derivative **2c** as superior antifouling candidates. These analogues distinguish themselves by striking a critical balance: they exhibit robust predicted binding affinity against key biofouling targets (GSK-3β, AChE, and BAM) while maintaining a safety profile characterized by significantly improved LC_{50} values, rapid biodegradation, and non-persistence. These findings position them as a promising new class of eco-friendly antifouling agents suitable for further development.

Suggestion

Based on the findings of this study, it is recommended that future work focus on validating the antifouling potential of the glucuronidated macrolactin A analogues (1a–1c) and the hydroxylated derivative 2c through comprehensive in vitro and in vivo experimentation. Further structure–activity relationship (SAR) optimization should also be considered to enhance their efficacy, biodegradability, and environmental stability. Expanding toxicity assessments across diverse marine species will be essential to ensure ecological safety and to evaluate long-term environmental impact.

http://ejournal.unsrat.ac.id/index.php/platax 10.35800/jipv10i2.65278

In addition, pilot-scale synthesis, formulation development, and field-based antifouling performance testing are strongly encouraged to determine real-world applicability. Complementary computational approaches, such as advanced molecular dynamics simulations and broader virtual screening of macrolactin derivatives, may further refine candidate selection and accelerate the development of a robust pipeline of eco-friendly antifouling agents.

ACKNOWLEDGEMENTS

The authors are grateful to the Indonesian Ministry of Higher Education, Science, and Technology for financial support (No. 182/C3/DT.05.00/PL-BATCH II/2025).

REFERENCE

Armstrong, R. A. (2014, September 1). When to use the Bonferroni correction. *Ophthalmic & Physiological Optics: The Journal of the British College of Ophthalmic Opticians (Optometrists)*, Vol. 34, pp. 502–508. https://doi.org/10.1111/opo.12131

Ayesu, E. K. (2023). Does shipping cause environmental emissions? Evidence from African countries. *Transportation Research Interdisciplinary Perspectives*, *21*. https://doi.org/10.1016/j.trip.2023.100873

Balansa, W., Rieuwpassa, F. J., & Hanif, N. (2025). *Harnessing Ecofriendly Antifouling of Agelasine Alkaloids*. Kamiya Jaya Aquatic.

Balansa, W., Riyanti, Balansa, K. H., & Hanif, N. (2025). Harnessing the Ecofriendly Antifouling Potential of Agelasine Alkaloids Through MetaTox Analysis and Computational Studies. *Tropical Journal of Natural Product Research*, *9*(1), 329–340. https://doi.org/10.26538/tjnpr/v9i1.42

Balansa, W., Riyanti, Manurung, U. N., Tomasoa, A. M., Hanif, N., Rieuwpassa, F. J., & Schäberle, T. F. (2024). Sponge-Based Ecofriendly Antifouling: Field Study on Nets, Molecular Docking with Agelasine Alkaloids. *Tropical Journal of Natural Product Research*, *8*(1), 5913–5924. https://doi.org/10.26538/tjnpr/v8i1.29

Balansa, W., Riyanti, Patras, M. A., Balansa, K. H., Hanif, N., Rieuwpassa, F. J., … Schäberle, T. F. (2025). Harnessing the metabolites from the marine sponge Melophlus sarasinorum for the discovery of eco-friendly antifoulants. *Biodiversitas*, *26*(4), 1590–1606. https://doi.org/10.13057/biodiv/d260411

Balansa, W., Riyanti, Rieuwpassa, F. J., & Hanif, N. (2025). *Harnessing ecofriendly antifouling of Agelasine alkaloids*. Kamija Aquatic.

Bannister, J., Sievers, M., Bush, F., & Bloecher, N. (2019). Biofouling in marine aquaculture: a review of recent research and developments. *Biofouling*, *35*(6), 631–648. https://doi.org/10.1080/08927014.2019.1640214

Cai, Y., Apell, J. N., Pflug, N. C., McNeill, K., & Bollmann, U. E. (2021). Photochemical fate of medetomidine in coastal and marine environments. *Water Research*, *191*, 116791. https://doi.org/https://doi.org/10.1016/j.watres.2020.116791

Card, M. L., Gomez-Alvarez, V., Lee, W.-H., Lynch, D. G., Orentas, N. S., Lee, M. T., … Boethling, R. S. (2017). History of EPI SuiteTM and future perspectives on chemical property estimation in US Toxic Substances Control Act new chemical risk assessments. *Environ. Sci.: Processes Impacts*, *19*(3), 203–212. https://doi.org/10.1039/C7EM00064B

Chadha, A., Padhi, S. K., Stella, S., Venkataraman, S., & Saravanan, T. (2024). Microbial alcohol dehydrogenases: recent developments and applications in asymmetric synthesis. *Org. Biomol. Chem.*, *22*(2), 228–251. https://doi.org/10.1039/D3OB01447A

Chen, Jiamin, Liu, T., Wei, M., Zhu, Z., Liu, W., & Zhang, Z. (2019). Macrolactin a

is the key antibacterial substance of Bacillus amyloliquefaciens D2WM against the pathogen Dickeya chrysanthemi. *European Journal of Plant Pathology*, *155*(2), 393–404. https://doi.org/10.1007/s10658-019-01774-3

Chen, Jipeng, Bai, W., Jian, R., Lin, Y., Zheng, X., Wei, F., … Xu, Y. (2024). Molecular structure design of polybenzoxazines with low surface energy and low modulus for marine antifouling application. *Progress in Organic Coatings*, *187*, 108165. https://doi.org/https://doi.org/10.1016/j.porgcoat.2023.108165

Chen, Jipeng, Zhao, J., Lin, F., Zheng, X., Jian, R., Lin, Y., … Xu, Y. (2023). Polymerized tung oil toughened urushiol-based benzoxazine copper polymer coatings with excellent antifouling performances. *Progress in Organic Coatings*, *177*, 107411. https://doi.org/https://doi.org/10.1016/j.porgcoat.2023.107411

Chen, L, & Qian, P. Y. (2017). The cardiac drug digoxin is a potent antifoulant against the barnacle Amphibalanus amphitrite. *J Mar Sci Eng. 2017;5(4):46*, *5*(4), 46.

Chen, Lianguo, & Qian, P. Y. (2017). Review on molecular mechanisms of antifouling compounds: An update since 2012. *Marine Drugs*, *15*(264), 1–20. https://doi.org/10.3390/md15090264

Coughtrie, M. W. H. (2016). Function and organization of the human cytosolic sulfotransferase (SULT) family. *Chemico-Biological Interactions*, *259*, 2–7. https://doi.org/https://doi.org/10.1016/j.cbi.2016.05.005

Dallakyan, S., & Olson, A. J. (2015). Small-Molecule Library Screening by Docking with PyRx. In J. E. Hempel, C. H. Williams, & C. C. Hong (Eds.), *Chemical Biology: Methods and Protocols* (pp. 243–250). New York, NY: Springer New York. https://doi.org/10.1007/978-1-4939-2269-7_19

Dixon-Clarke, S. E., Elkins, J. M., Cheng, S. W. G., Morin, G. B., & Bullock, A. N. (2015). Structures of the CDK12/CycK complex with AMP-PNP reveal a flexible C-terminal kinase extension important for ATP binding. *Scientific Reports*, *5*. https://doi.org/10.1038/srep17122

Dobretsov, S., & Rittschof, D. (2023, July 1). “Omics” Techniques Used in Marine Biofouling Studies. *International Journal of Molecular Sciences*, Vol. 24. Multidisciplinary Digital Publishing Institute (MDPI). https://doi.org/10.3390/ijms241310518

Docampo-Palacios, M. L., Alvarez-Hernández, A., Adiji, O., Gamiotea-Turro, D., Valerino-Diaz, A. B., Viegas, L. P., … Dixon, R. A. (2020). Glucuronidation of Methylated Quercetin Derivatives: Chemical and Biochemical Approaches. *Journal of Agricultural and Food Chemistry*, *68*(50), 14790–14807. https://doi.org/10.1021/acs.jafc.0c04500

Escher, B. I., & Schwarzenbach, R. P. (2002). Conflicting toxicological goals: Degradation versus bioaccumulation of organic compounds. *Environmental Science & Technology*, *36*(16), 3505–3511.

Farkas, A., Degiuli, N., Martić, I., & Vujanović, M. (2021). Greenhouse gas emissions reduction potential by using antifouling coatings in a maritime transport industry. *Journal of Cleaner Production*, *295*, 126428. https://doi.org/https://doi.org/10.1016/j.jclepro.2021.126428

Fiorucci, S., Carino, A., Baldoni, M., Santucci, L., Costanzi, E., Graziosi, L., … Biagioli, M. (2021, March 1). Bile Acid Signaling in Inflammatory Bowel Diseases. *Digestive Diseases and Sciences*, Vol. 66, pp. 674–693. Springer. https://doi.org/10.1007/s10620-020-06715-3

Gagan, J., & et al. (2012). UDP-Glucuronosyltransferases: A family of enzymes essential in drug

metabolism and detoxification. *Drug Metabolism and Disposition*, *40*(6), 1051–1065.

Georgiades, E., Scianni, C., Davidson, I., Tamburri, M. N., First, M. R., Ruiz, G., … Kluza, D. (2021). The Role of Vessel Biofouling in the Translocation of Marine Pathogens: Management Considerations and Challenges. *Frontiers in Marine Science*, *8*. https://doi.org/10.3389/fmars.2021.660125

Graziani, E. I., Cane, D. E., Betlach, M. C., Kealey, J. T., & McDaniel, R. (1998). Macrolide biosynthesis: A single cytochrome P450, PicK, is responsible for the hydroxylations that generate methymycin, neomethymycin, and picromycin in Streptomyces venezuelae. *Bioorganic & Medicinal Chemistry Letters*, *8*(22), 3117–3120. https://doi.org/https://doi.org/10.1016/S0960-894X(98)00553-8

Gu, Y., Li, H., Dong, H., Zeng, Y., Zhang, Z., Paterson, N. G., … Dong, C. (2016). Structural basis of outer membrane protein insertion by the BAM complex. *Nature*, *531*(7592), 64–69. https://doi.org/10.1038/nature17199

Guglya, E. B., Belozerova, O. A., Shikov, A. E., Alferova, V. A., Romanenko, M. N., Chebotar, V. K., … Terekhov, S. S. (2025). Bacillus-Based Biocontrol Agents Mediate Pathogen Killing by Biodegradable Antimicrobials from Macrolactin Family. *International Journal of Molecular Sciences*, *26*(22), 11167. https://doi.org/10.3390/ijms262211167

Gumbart, J. C., & et al. (2019). Molecular dynamics simulations of the bacterial outer membrane protein insertion machinery BAM complex. *Journal of Biological Chemistry*, *294*(50), 19087–19097.

Hinonaung, J. S. H., Tinungki, Y. L., & Balansa, W. (2025). Structure-Based Discovery of Immunomodulators for Stunting Inspired by Caulerpin: A Rational Approach Targeting Immune Homeostasis. *Tropical Journal of Natural Product Research*, *9*(9). https://doi.org/10.26538/tjnpr/v9i9.45

Jaramillo, M. O., & et al. (2021). Macrolactin A as a novel inhibitory agent for SARS-CoV-2 Mpro. *Frontiers in Chemistry, 9, . [PMID:]* , *9*(715568).

Järvinen, E., Deng, F., Kiander, W., Sinokki, A., Kidron, H., & Sjöstedt, N. (2022, January 13). The Role of Uptake and Efflux Transporters in the Disposition of Glucuronide and Sulfate Conjugates. *Frontiers in Pharmacology*, Vol. 12. Frontiers Media S.A. https://doi.org/10.3389/fphar.2021.802539

Kaur, H., Jakob, R. P., Marzinek, J. K., Green, R., Imai, Y., Bolla, J. R., … Hiller, S. (2021). The antibiotic darobactin mimics a β-strand to inhibit outer membrane insertase. *Nature*, *593*(7857), 125–129. https://doi.org/10.1038/s41586-021-03455-w

Kim, J. A., Choi, S. S., Lim, J. K., & Kim, E. S. (2025, April 25). Unlocking marine treasures: isolation and mining strategies of natural products from sponge-associated bacteria. *Natural Product Reports*, Vol. 42, pp. 1195–1225. Royal Society of Chemistry. https://doi.org/10.1039/d5np00013k

Kim, T. H., & et al. (2014). Anti-settlement activity of marine natural products from a red algae, Laurencia undulata, against the barnacle Balanus amphitrite. *Journal of Applied Phycology*, *26*(1), 503–511.

Lee, Y., Yoon, S. B., Hong, H., Kim, H. Y., Jung, D., Moon, B. S., … Cho, H. (2022). Discovery of GSK3β Inhibitors through In Silico Prediction-and-Experiment Cycling Strategy, and Biological Evaluation. *Molecules*, *27*(12). https://doi.org/10.3390/molecules27123825

Luque, F. J., & Muñoz-Torrero, D. (2023). Acetylcholinesterase: A Versatile Template to Coin Potent Modulators of Multiple Therapeutic Targets. *Accounts of Chemical Research*.

https://doi.org/10.1021/acs.accounts.3c00617

Ma, Z., Ajibade, A., & Zou, X. (2024). Docking strategies for predicting protein-ligand interactions and their application to structure-based drug design. *Communications in Information and Systems*, *24*(3), 199–230. https://doi.org/10.4310/CIS.241021221101

Mondol, Mohamad Abdul Mojid, Tareq, F. S., Kim, J. H., Lee, M. A., Lee, H. S., Lee, J. S., … Shin, H. J. (2013, February). New antimicrobial compounds from a marine-derived Bacillus sp. *Journal of Antibiotics*, Vol. 66, pp. 89–95. https://doi.org/10.1038/ja.2012.102

Mondol, Muhammad Abdul Mojid, & Shin, H. J. (2014). Antibacterial and antiyeast compounds from marine-derived bacteria. *Marine Drugs*, *12*(5), 2913–2921. https://doi.org/10.3390/md12052913

Nagao, T., Adachi, K., Sakai, M., Nishijima, M., & Sanoll, H. (2001). Novel Macrolactins as Antibiotic Lactones from a Marine Bacterium. *The Journal of Antibiotics*, *54*(4), 333–339.

Norouzi, S., Nahmiach, N., Perez, G., Zhu, Y., Peslherbe, G. H., Muir, D. C. G., & Zhang, X. (2025). Molecular docking for screening chemicals of environmental health concern: insight from a case study on bisphenols. *Environmental Science: Processes & Impacts*. https://doi.org/10.1039/d5em00084j

Nyström, B., Becker-Van Slooten, K., Bérard, A., Grandjean, D., Druart, J.-C., & Leboulanger, C. (2002). Toxic effects of Irgarol 1051 on phytoplankton and macrophytes in Lake Geneva. *Water Research*, *36*(8), 2020–2028. https://doi.org/https://doi.org/10.1016/S0043-1354(01)00404-3

Ohji, M., Harino, H., Hayashizaki, K., Yusoff, F. Md., & Inoue, K. (2023). Bioaccumulation of antifouling biocides in mangroves and seagrasses in coastal ecosystems. *Journal of the Marine Biological Association of the United Kingdom*, *103*, e24. https://doi.org/DOI: 10.1017/S0025315423000024

Olick, D. (2023, October 30). Shipping industry could lose $10 billion a year battling climate change by 2050. Retrieved November 25, 2025, from CNBC website: https://www.cnbc.com/diana-olick/

Onuh, A. C., Manopaek, R., Vangnai, A. S., Tiyayon, P., & Vinayavekhin, N. (2025). Ralstonia solanacearum Secretions Induce Shifts in Macrolactin Composition and Reduction in Antimicrobial Activity of Bacillus amyloliquefaciens BNC5. *Journal of Agricultural and Food Chemistry*, *73*(20), 12525–12536. https://doi.org/10.1021/acs.jafc.5c03489

Ortiz, A., & Sansinenea, E. (2020). Macrolactin Antibiotics: Amazing Natural Products. *Mini-Reviews in Medicinal Chemistry*, *20*(7), 584–600. https://doi.org/10.2174/1389557519666191205124050

Pan, L. lu, Yang, Y., Hui, M., Wang, S., Li, C. yun, Zhang, H., … Zhong, D. fang. (2021). Sulfation predominates the pharmacokinetics, metabolism, and excretion of forsythin in humans: major enzymes and transporters identified. *Acta Pharmacologica Sinica*, *42*(2), 311–322. https://doi.org/10.1038/s41401-020-0481-8

Puniya, B. L. (2025, September 1). Artificial-intelligence-driven Innovations in Mechanistic Computational Modeling and Digital Twins for Biomedical Applications. *Journal of Molecular Biology*, Vol. 437. Academic Press. https://doi.org/10.1016/j.jmb.2025.169181

Qian, P. Y., Chen, L., & Xu, Y. (2013). Mini-review: Molecular mechanisms of antifouling compounds. *Biofouling*, Vol. 29, pp. 381–400. Taylor and Francis Ltd. https://doi.org/10.1080/08927014.2013.776546

Qian, P.-Y., Xu, Y., & Fusetani, N. (2010). Natural products as antifouling compounds: recent progress and future perspectives. *Biofouling*, *26*(2), 223–234. https://doi.org/10.1080/08927010903470815

Qiao, L., Dong, Y., Zhou, H., & Cui, H. (2023). *Effect of Post-Polyketide Synthase Modification Groups on Property and Activity of Polyene Macrolides*. https://doi.org/10.3390/antibiotics

Qing, F. D., Qiu, Y., Wang, W., Wang, X., Qang Ouyang, P., & Huan Ke, C. (2013). Antifouling activities of hymenialdisine and debromohymenialdisine from the sponge Axinella sp. *International Biodeterioration & Biodegradation*, *85*, 359–364. https://doi.org/https://doi.org/10.1016/j.ibiod.2013.08.014

Rittschof, D. (2001). Natural antifoulants and coatings: Marine antifouling in an environmentally friendly way. *Journal of Coatings Technology*, *73*(919), 75–81.

Riyanti, Marner, M., Hartwig, C., Patras, M. A., Wodi, S. I. M., Rieuwpassa, F. J., … Schäberle, T. F. (2020). Sustainable Low-Volume Analysis of Environmental Samples by Semi-Automated Prioritization of Extracts for Natural Product Research (SeaPEPR). *Marine Drugs*, *18*(12). https://doi.org/10.3390/md18120649

Sathiyanarayanan, G., Saibaba, G., Kiran, G. S., Yang, Y.-H., & Selvin, J. (2017). Marine sponge-associated bacteria as a potential source for polyhydroxyalkanoates. *Critical Reviews in Microbiology*, *43*(3), 294–312. https://doi.org/10.1080/1040841X.2016.1206060

Selim, M. S., Shenashen, M. A., El-Safty, S. A., Higazy, S. A., Selim, M. M., Isago, H., & Elmarakbi, A. (2017). Recent progress in marine foul-release polymeric nanocomposite coatings. *Progress in Materials Science*, *87*, 1–32. https://doi.org/https://doi.org/10.1016/j.pmatsci.2017.02.001

Song, S., De Marco Muscat-Fenech, C., & Demirel, Y. K. (2021). Economic and environmental impacts of different antifouling strategies for fishing boats in Turkey. *In: 2nd International Conference on Ship and Marine Technology*. Retrieved from https://www.gmoshipmar.org/GMOSHIPMAR2021

Song, Y., Zhou, Y., Cong, M., Deng, S., Chen, Y., Pang, X., … Wang, J. (2024). New 24-Membered Macrolactines from an Arctic Bacterium Bacillus amyloliquefaciens SCSIO 41392 and Their Anti-Pathogenicity Evaluation. *Marine Drugs*, *22*(11). https://doi.org/10.3390/md22110484

Sun, L., Van Loey, A., Buvé, C., & Michiels, C. W. (2023). Experimental Evolution Reveals a Novel Ene Reductase That Detoxifies α,β-Unsaturated Aldehydes in Listeria monocytogenes. *Microbiology Spectrum*, *11*(3). https://doi.org/10.1128/spectrum.04877-22

Tornio, A., Filppula, A. M., Kailari, O., Neuvonen, M., Nyrönen, T. H., Tapaninen, T., … Backman, J. T. (2014). Glucuronidation Converts Clopidogrel to a Strong Time-Dependent Inhibitor of CYP2C8: A Phase II Metabolite as a Perpetrator of Drug–Drug Interactions. *Clinical Pharmacology & Therapeutics*, *96*(4), 498–507. https://doi.org/https://doi.org/10.1038/clpt.2014.141

Vedaprakash, L., Senthilkumar, P., Inbakandan, D., & Venkatesan, R. (2022). Marine Biofouling and Corrosion on Long-Term Behavior of Marine Structures. In U. Kamachi Mudali, T. Subba Rao, S. Ningshen, R. G. Pillai, R. P. George, & T. M. Sridhar (Eds.), *A Treatise on Corrosion Science, Engineering and Technology* (pp. 447–466). Singapore: Springer Nature Singapore.

https://doi.org/10.1007/978-981-16-9302-1_24

Wang, K. L., Wu, Z. H., Wang, Y., Wang, C. Y., & Xu, Y. (2017, September 1). Mini-review: Antifouling natural products from marine microorganisms and their synthetic analogs. *Marine Drugs*, Vol. 15. MDPI AG. https://doi.org/10.3390/md15090266

Wishart, D. S., Tian, S., Allen, D., Oler, E., Peters, H., Lui, V. W., … Metz, T. O. (2022). BioTransformer 3.0 - a web server for accurately predicting metabolic transformation products. *Nucleic Acids Research*, *50*(W1), W115–W123. https://doi.org/10.1093/nar/gkac313

Wu, T., Xiao, F., & Li, W. (2021, February 1). Macrolactins: biological activity and biosynthesis. *Marine Life Science and Technology*, Vol. 3, pp. 62–68. Springer. https://doi.org/10.1007/s42995-020-00068-6

Wu, W. Y., Dai, Y. C., Li, N. G., Dong, Z. X., Gu, T., Shi, Z. H., … Duan, J. A. (2017, June 28). Novel multitarget-directed tacrine derivatives as potential candidates for the treatment of alzheimer's disease. *Journal of Enzyme Inhibition and Medicinal Chemistry*, Vol. 32, pp. 572–587. Taylor and Francis Ltd. https://doi.org/10.1080/14756366.2016.1210139

Xu, Y., Song, Y., Ning, Y., Li, S., Qu, Y., Jiao, B., & Lu, X. (2024). Macrolactin XY, a Macrolactin Antibiotic from Marine-Derived Bacillus subtilis sp. 18. *Marine Drugs*, *22*(8). https://doi.org/10.3390/md22080331

Yousef, A. N. A. (2023). Examining the effects of bio fouling on ships and how it contributes to the introduction of non-native species in newly discovered coastal areas in "Bio fouling on Ship Hulls and Its Ecological Ramification Abdel Nasser alsheikh Yousef. *SSRN*, 1–26. https://doi.org/https://dx.doi.org/10.2139/ssrn.4666557

Zieliński, M., Park, J., Sleno, B., & Berghuis, A. M. (2021). Structural and functional insights into esterase-mediated macrolide resistance. *Nature Communications*, *12*(1). https://doi.org/10.1038/s41467-021-22016-3

Zuo, L., & et al. (2023). Macrolactin A is an inhibitor of protein biosynthesis in bacteria. *Antimicrobial Agents and Chemotherapy*, *67*(11), e00305–e00323.